NMR Spectroscopy

International Edition: DOI: 10.1002/anie.201610759
German Edition: DOI: 10.1002/ange.201610759

# Separating Dipolar and Chemical Exchange Magnetization Transfer Processes in $^1$H-CEST

*Tairan Yuwen, Ashok Sekhar, and Lewis E. Kay**

***Abstract:*** *An amide $^1$H-Chemical Exchange Saturation Transfer (CEST) experiment is presented for studies of conformational exchange in proteins. The approach, exploiting spin-state-selective magnetization transfer, completely suppresses undesired NOE-based dips in CEST profiles so that chemical exchange processes can be studied. The methodology is demonstrated with applications involving proteins that interconvert on the millisecond timescale between major and invisible minor states, and accurate amide $^1$H chemical shifts of the minor conformer are obtained in each case. The spin-state-selective magnetization transfer approach offers unique possibilities for quantitative studies of protein exchange through $^1$H-CEST.*

The interconversion between different conformers can be critically important in a range of biological processes including protein folding and misfolding, enzyme function, and ligand binding.[1] Solution NMR has emerged as an important tool for characterizing the kinetics and thermodynamics of biomolecular interconversion and for generating atomic resolution models of the conformational states that are visited during the exchange event.[1b] One particular approach, chemical exchange saturation transfer (CEST),[2] has recently gained importance in studies of biomolecular conformational exchange between visible major (ground, $G$) and invisible minor (excited, $E$) states, $G \underset{k_{EG}}{\overset{k_{GE}}{\rightleftharpoons}} E$, so long as the rate of interconversion is in the 50–400 $s^{-1}$ range and the fractional population of $E$, $p_E$, is in excess of $\approx 0.5\,\%$. CEST experiments offer an alternative to CPMG-based studies of conformational exchange, especially for slowly exchanging systems where dispersion profiles are typically small. For example, for $p_E = 2\,\%$, $k_{ex} = k_{GE} + k_{EG} = 100\ s^{-1}$ dispersion profiles are less than $2\ s^{-1}$, yet large CEST effects are observed.[2a] Initial applications of the methodology in the 1970s focused on $^1$H-CEST to assign resonances of highly populated interconverting conformers to individual molecular species,[3] yet relatively few examples have been reported over the years. A significant limitation of the $^1$H-CEST experiment has always been the difficulty in separating exchange from $^1$H–$^1$H dipolar (NOE) effects and for proteins, where a high density of protons ensures a large number of dipolar pathways, NOEs can mask exchange peaks in spectra.[4] This problem was partially addressed for amide protons, and in particular for measuring amide $^1$H chemical shifts in state $E$, by recording a series of $^{15}$N-CEST profiles as a function of the position of a $^1$H-CW decoupling field.[4] Resonance positions of excited state protons were obtained indirectly through one-bond $^1$H–$^{15}$N splittings of the corresponding excited state CEST dips, because these depend on the displacement between the $^1$H shift and the known position of the decoupling field.[5] Despite some success with this approach, large $^{15}$N shift differences between ground and excited state peaks ($\Delta\varpi_N$) are required, and because $\Delta\varpi_H$ and $\Delta\varpi_N$ are often uncorrelated, the utility of this method is limited. Alternatively, $^1$H-CEST experiments based on longitudinal order, rather than on longitudinal magnetization, can be recorded that take advantage of favorable boundary conditions that reduce the sizes of NOE dips in CEST profiles.[6] Yet for moderate to large proteins, the NOE effect is still prohibitive and the appeal of the method is further reduced by the fact that its intrinsic sensitivity is less than for longitudinal magnetization based experiments because of the more rapid relaxation of longitudinal order. Thus, the vast majority of CEST experiments applied to biomolecular systems focus on $^{15}$N and $^{13}$C nuclei that, owing to their significantly lower gyromagnetic ratios, do not produce NOE dips in profiles.

Despite the utility of $^{15}$N- and $^{13}$C-CEST, the possibility of recording $^1$H-CEST experiments is still of interest as $^1$H spins are sensitive probes of conformational exchange. We have therefore revisited the problem and present here a $^1$H-based CEST experiment that separates chemical and dipolar exchange effects to produce CEST profiles that are free from NOEs. The utility of the approach is demonstrated on a pair of exchanging protein systems, focusing on amide protons, but in principle it can be applied to other protons, such as those on methyl groups.

Figure 1 A shows a $^1$H-CEST profile that was simulated using a pair of dipolar-coupled protons, $I$ and $S$, that are, in turn, one-bond scalar coupled to $^{15}$N spins, in a system exchanging between states $G$ and $E$. The profile of only one of the protons, $I$, is highlighted, showing both CEST and NOE dips. Such a profile would be obtained from a CEST experiment in which the CEST element is placed immediately prior to an $^{15}$N,$^1$H-HSQC read-out scheme, with the intensity of proton $I$ (state $G$) obtained from the corresponding $I$ cross-peak in spectra measured as a function of the position of the weak $^1$H $B_1$ field. Major and minor dips are observed at 0.0 ppm and 1.0 ppm for proton $I$ in states $G$ and $E$,

[*] Dr. T. Yuwen, Dr. A. Sekhar, Prof. L. E. Kay
Departments of Molecular Genetics, Biochemistry, and Chemistry
University of Toronto
Toronto, Ontario M5S 1A8 (Canada)
E-mail: kay@pound.med.utoronto.ca
Prof. L. E. Kay
Hospital for Sick Children
Program in Molecular Structure and Function
555 University Avenue, Toronto, Ontario M5G 1X8 (Canada)
Supporting information and the ORCID identification number(s) for the author(s) of this article can be found under http://dx.doi.org/10.1002/anie.201610759.

  

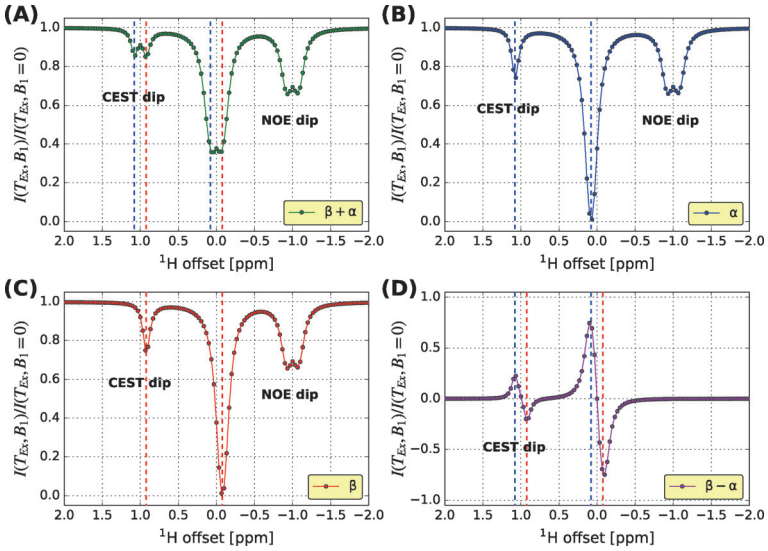


***Figure 1.*** Simulated $^1$H-CEST profiles showing chemical exchange (CEST) and NOE dips and their separation using experiments that exploit the spin-state of the attached heteroatom. Each profile was generated for a pair of dipolar-coupled amide protons that in turn are scalar coupled to $^{15}$N spins. $I(T_{Ex},B_1)$ and $I(T_{Ex},B_1=0)$ are intensities of peak $I$ with and without the CEST $B_1$ field, respectively. A) $^1$H-CEST profile generated in a typical CEST experiment that does not involve spin-state-selective magnetization transfers. B, C) $^1$H-CEST profiles from $IN^{I\alpha}$ (B) and $IN^{I\beta}$ (C) pathways. Note the offset of the major and minor CEST dips, but not of the NOE dips, in the two traces. D) Difference profile, $IN^{I\beta}-IN^{I\alpha}$, that removes the NOE dips. The simulation (Supporting Information) was based on the following parameters: $k_{ex}=200\ s^{-1}$, $p_E=2\%$, cross relaxation rate $\sigma=-2\ s^{-1}$, $T_{Ex}=400$ ms, $\Delta\varpi=1.0$ ppm and $-1.0$ ppm for CEST and NOE dips, respectively, $B_1$ (CEST) $=20$ Hz, $^1J_{HN}=-93$ Hz. $B_1$ inhomogeneity has been taken into account as described previously.[2a] Positions of ground and excited state chemical shifts are indicated by dashed lines.

respectively, while the dip at $-1.0$ ppm corresponds to the resonance frequency of proton *S*. Notably, each of the dips is split into a doublet owing to one-bond $^1$H–$^{15}$N scalar couplings, as $^{15}$N-decoupling is not applied during the $^1$H-CEST period. In the general case, using a simple HSQC-based readout, it is not possible to establish whether two chemical exchange processes are operative, resulting in a pair of minor dips, or whether both minor dips are due to NOEs, or, in the case where both exchange and dipolar magnetization transfer are operative, which of the two dips corresponds to each process.

A solution to this problem is realized by exploiting the spin-state of the attached heteroatom, $^{15}$N in this case, and noting that the behavior of spin-state-selective $^1$H longitudinal magnetization is different for CEST and NOE transfers. This difference provides an avenue for the separation of the two effects, as illustrated in Figures 1 B,C using the same spin system as in Figure 1 A. Here, we consider a system (see below) whereby, immediately after the CEST element of duration $T_{Ex}$, amide proton magnetization from spin *I* coupled to the attached $^{15}$N in the up state ($N^{I\alpha}$, Figure 1 B) is transferred to the $^{15}$N-TROSY component[7] and then subsequently to the $^1$H-TROSY line.[8] In a second experiment, magnetization from spin *I* coupled to $N^{I\beta}$ is selected and transferred in the same manner through a spin-state-selective pathway that uses the TROSY component exclusively as well. The pathways give rise to a pair of CEST profiles that will be referred to in what follows as $IN^{I\alpha}$ and $IN^{I\beta}$. In a typical implementation, $^{15}$N ($N_xI^\beta$) and $^1$H ($I_xN^\beta$) chemical shift evolution would be recorded to generate a 2D-TROSY-based HSQC dataset.[8] Profiles similar to those in Figures 1 B,C are obtained by plotting the intensity of the TROSY peak in HSQC spectra, $I(T_{Ex})$, as a function of the position of the $^1$H-CEST field that is placed at a different frequency in each of a series of 2D data sets. A comparison of Figures 1 B,C establishes that the key difference in the profiles lies in the positions of both the CEST minor and major dips, with a relative shift of $^1J_{HN}$, the one-bond $^1$H–$^{15}$N scalar coupling. This arises because chemical exchange between corresponding *I* spins in *G* and *E* does not affect the attached $^{15}$N spin states so that, for large $^{15}$N $T_1$ values (see the Supporting Information), one can think of each chemical exchange event as involving two separate pathways that are distinguished by the spin state of $N^I$. Separate CEST profiles are obtained because *I* magnetization associated with each of the different $^{15}$N spin-states is selected independently after the CEST element in each of two schemes. In contrast, the NOE dip derives from dipolar magnetization transfer from spin *S* to spin *I*, and this transfer occurs i) in a manner that is independent of the spin-state of $N^S$, the $^{15}$N spin that is one bond coupled to *S*, and ii) affects both spin-state-selective components of *I* magnetization equally. Selection of either the $IN^{I\alpha}$ or $IN^{I\beta}$ pathways leads, therefore, to profiles with exactly the same doublet structure for the NOE peak, centered at the resonance position of spin *S*. Subsequently, subtraction of $IN^{I\alpha}$ from $IN^{I\beta}$ (profile C−profile B) gives the profile shown in Figure 1 D with the NOE dip eliminated and where both major and minor dips that report on the chemical exchange process have an approximate anti-phase absorptive lineshape (see the Supporting Information).

Figure 2 illustrates the TROSY-based pulse scheme that has been developed for measuring amide $^1$H-CEST in exchanging biomolecular systems. Central to the scheme is the ST2 element[7] immediately following the $^1$H-CEST period of duration $T_{Ex}$ that transfers *I* magnetization in a spin-state-selective manner to the $^{15}$N-TROSY component ($t_1$ evolution) and then subsequently to transverse *I* proton magnetization (TROSY component) for detection, following

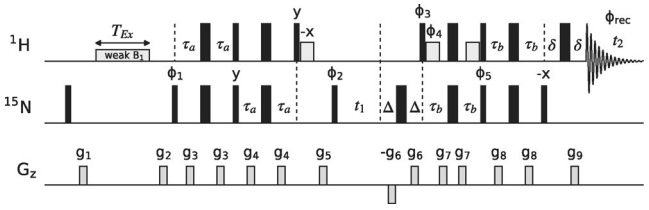


***Figure 2.*** TROSY version of the amide $^1$H-CEST pulse scheme. The corresponding sequence for studies of small proteins is given in Figure S1.

  

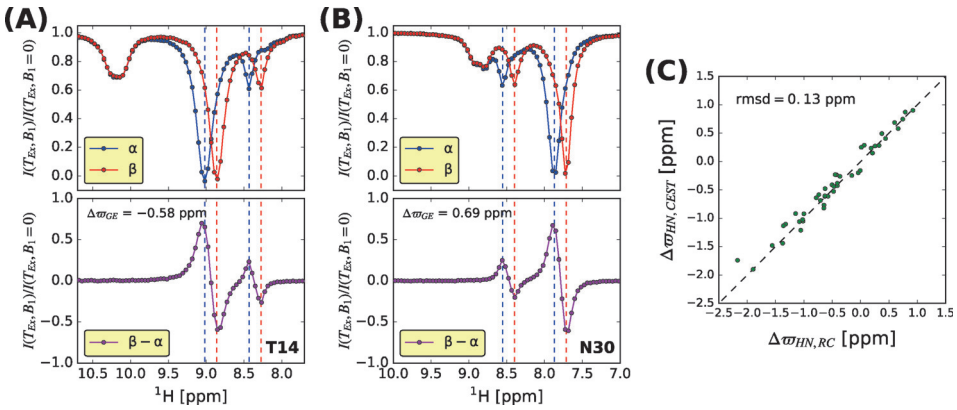


***Figure 3.*** A, B) Amide $^1$H-CEST profiles for T14 (A) and N30 (B) of G48A Fyn SH3 measured with the non-TROSY scheme of Figure S1, 11 °C, $T_{Ex}$ = 400 ms, 600 MHz. Top) Superposition of $IN^{I\alpha}$ (blue) and $IN^{I\beta}$ (red) pathways. Bottom) Difference profile that eliminates the NOE dips. C) Correlation of $^1$H $\Delta\varpi_{GE}$ values obtained from $^1$H-CEST (*y*-axis) with those predicted assuming random coil chemical shifts (*x*-axis) using the method of Tamiola et al.[13]

the scheme of Pervushin and co-workers.[8] The experiment is well-suited for studies of high molecular weight proteins; in applications to small proteins, a different version of the experiment, in which the HSQC-read element is non-TROSY, may be desirable (Figure S1).

To illustrate the utility of the methodology, we first considered the G48A Fyn SH3 domain that interconverts between a highly populated folded state and a sparsely populated unfolded ensemble.[9] Figures 3 A, B show amide $^1$H-CEST profiles derived from spin-state-selective magnetization transfers for T14 (A) and N30 (B) recorded on a highly deuterated, $^{15}$N-labeled sample of G48A Fyn SH3 with the scheme of Figure S1, using a CEST element of duration 400 ms and a $^1$H-CEST field of 25 Hz, 11 °C. Both $IN^{I\alpha}$ and $IN^{I\beta}$ profiles are effectively scaled to 1, as described in the Supporting Information. Notably, we have observed little difference in amide $^1$H longitudinal spin-state relaxation rates, on the order of 0.02 $s^{-1}$ for the protein systems considered here, reflecting the small contribution from cross-correlated relaxation involving $^1$H–$^{15}$N dipolar/$^1$H CSA interactions (scales as $1/\omega_H^2$, where $\omega_H$ is the $^1$H Larmor frequency, rad $s^{-1}$). Despite the small size of this domain (7 kDa), NOE dips that are as large as CEST dips are observed that complicate analysis of the data (A, B, top). Yet the difference profiles obtained from subtracting the spin-state-selective CEST profiles (A, B, bottom) are free of NOE dips and can be readily fit to extract $\Delta\varpi_{GE}$ values (Supporting Information). Figure 3 C shows that an excellent correlation is observed between extracted amide $^1$H shift differences and those predicted assuming that the amide shifts of the unfolded ensemble are those of a random coil (rmsd = 0.13 ppm). The extracted ($p_E$, $k_{ex}$) values of (5.3 ± 0.2 %, 36.4 ± 1.3 $s^{-1}$), obtained from fits of $^1$H-CEST profiles recorded with $B_1$ fields of 25 and 40 Hz, are in good agreement with (5.4 ± 0.1 %, 32.5 ± 0.9 $s^{-1}$) measured from $^{15}$N-CEST experiments.

Having established the robustness of the method for small proteins, we next looked at a more challenging case, the L99A cavity mutant of T4 lysozyme (L99A T4L). L99A T4L interconverts between a ground state that contains a 150 Å$^3$ cavity caused by the replacement of Leu99 with Ala,[10] and a sparsely populated conformer where the cavity becomes occupied by Phe114.[11] At 25 °C, $k_{ex}$ is on the order of 1500 $s^{-1}$,[12] but at 9 °C the exchange rate is sufficiently slowed so that the interconversion process is amenable to CEST, ($p_E$, $k_{ex}$) = (1.8 ± 0.01 %, 215.1 ± 4.9 $s^{-1}$) measured by $^{15}$N-CEST. Figure 4 A–E highlights selected $IN^{I\alpha}$ and $IN^{I\beta}$ profiles obtained from an amide $^1$H-CEST experiment recorded on

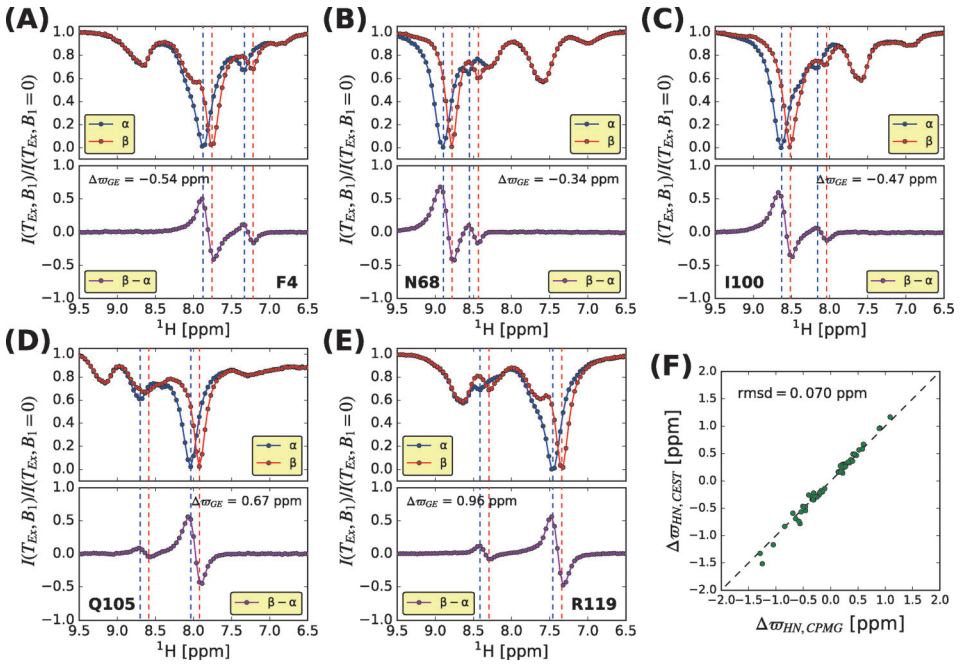


***Figure 4.*** A–E) Amide $^1$H-CEST profiles ($IN^{I\alpha}$ and $IN^{I\beta}$) for representative residues from L99A T4L, 9 °C, $T_{Ex}$ = 400 ms, 800 MHz, along with difference profiles. Positions of ground and excited state chemical shifts are indicated by dashed lines. F) Linear correlation plot of $\Delta\varpi_{GE}$ values obtained from $^1$H-CEST (*y*-axis) vs. those measured from $^1$H-CPMG experiments (*x*-axis) at 25 °C.[4]

a perdeuterated T4L sample, 9 °C with the scheme of Figure 2, $T_{Ex} = 400$ ms. Owing to the larger size and significantly slower tumbling time than for Fyn SH3 ($\approx 19$ ns vs. 6 ns), NOE dips are much more prevalent in this application and they obscure the CEST dips in both of the spin-state CEST profiles. Yet each of the difference profiles clearly shows a pair of CEST dips, from which $^1$H $\Delta\varpi_{GE}$ values can be robustly extracted. Figure 4F shows the excellent correlation between $^1$H shift differences extracted from CEST profiles, 9 °C, and the corresponding shift differences obtained from an analysis of $^1$H-CPMG data sets recorded at 25 °C.

It is worth noting that $^1$H-CEST experiments are best recorded on samples with high levels of deuteration. First, deuteration leads to smaller $^1$H spin relaxation rates, decreasing the losses that occur during coherence transfer steps, $^{15}$N frequency labeling and acquisition. Second, cross-relaxation involving a large bath of $^1$H spins decreases the size of the CEST dips associated with state $E$, as discussed in detail in the Supporting Infomration. For this reason it is not possible, in general, to obtain accurate exchange parameters ($p_E$, $k_{ex}$) from $^1$H-CEST experiments when NOE effects are large, as the smaller dip sizes lead to an underestimate of exchange parameters (Figures S2, S3). We thus recommend that $p_E$ and $k_{ex}$ be obtained using $^{15}$N- or $^{13}$C-based CEST experiments. In contrast, $^1$H $\Delta\varpi_{GE}$ values, which are the parameters of general interest, can be measured very accurately by $^1$H-CEST using a single experiment with a $B_1$ value that is optimal for the relevant exchange parameters (Figures S4–S6), as the present examples illustrate. Finally, the benefits from deuteration in the context of $^1$H-CEST experiments are also relevant for amide $^1$H-CPMG-based schemes where increased amide proton $T_2$ values, elimination of $^1$H–$^1$H scalar couplings and $^1$H-ROE effects produce higher quality $^1$H-CPMG profiles.[14]

In summary, we have presented spin-state-selective $^1$H-CEST experiments for measuring chemical shifts of amide protons in excited protein states. The experiments allow for the complete separation of NOE and chemical exchange dips so that CEST profiles are obtained that directly report on the exchange process of interest. The methodology can be applied to other protons in suitably labeled proteins. It significantly increases the utility of protein CEST for studies of invisible states by adding an additional nucleus to complement $^{15}$N and $^{13}$C spins that are already used as quantitative probes of invisible protein states in a range of applications.

## Acknowledgements

This work was funded through a Canadian Institutes of Health Research grant to L.E.K. L.E.K. holds a Canada Research Chair in Biochemistry. We are grateful to Dr. Guillaume Bouvignies for useful discussions.

## Conflict of interest

The authors declare no conflict of interest.

**Keywords:** amide protons · conformational dynamics · cross relaxation · proteins · proton CEST

**How to cite:** *Angew. Chem. Int. Ed.* **2017**, *56*, 6122–6125
*Angew. Chem.* **2017**, *129*, 6218–6221

[1] a) M. Karplus, J. Kuriyan, *Proc. Natl. Acad. Sci. USA* **2005**, *102*, 6679–6685; b) A. Sekhar, L. E. Kay, *Proc. Natl. Acad. Sci. USA* **2013**, *110*, 12867–12874; c) K. Henzler-Wildman, D. Kern, *Nature* **2007**, *450*, 964–972; d) D. D. Boehr, D. McElheny, H. J. Dyson, P. E. Wright, *Science* **2006**, *313*, 1638–1642; e) P. Neudecker, P. Robustelli, A. Cavalli, P. Walsh, P. Lundstrom, A. Zarrine-Afsar, S. Sharpe, M. Vendruscolo, L. E. Kay, *Science* **2012**, *336*, 362–366; f) N. J. Anthis, M. Doucleff, G. M. Clore, *J. Am. Chem. Soc.* **2011**, *133*, 18966–18974.

[2] a) P. Vallurupalli, G. Bouvignies, L. E. Kay, *J. Am. Chem. Soc.* **2012**, *134*, 8148–8161; b) N. J. Anthis, G. M. Clore, *Q. Rev. Biophys.* **2015**, *48*, 35–116.

[3] a) R. K. Gupta, A. G. Redfield, *Science* **1970**, *169*, 1204–1206; b) P. J. Cayley, J. P. Albrand, J. Feeney, G. C. K. Roberts, E. A. Piper, A. S. V. Burgen, *Biochemistry* **1979**, *18*, 3886–3895; c) E. I. Hyde, B. Birdsall, G. C. K. Roberts, J. Feeney, A. S. V. Burgen, *Biochemistry* **1980**, *19*, 3738–3746.

[4] G. Bouvignies, L. E. Kay, *J. Phys. Chem. B* **2012**, *116*, 14311–14317.

[5] R. Freeman, *Handbook of Nuclear Magnetic Resonance*, Wiley, New York, **1988**.

[6] A. Sekhar, R. Rosenzweig, G. Bouvignies, L. E. Kay, *Proc. Natl. Acad. Sci. USA* **2016**, *113*, E2794–E2801.

[7] K. V. Pervushin, G. Wider, K. Wuthrich, *J. Biomol. NMR* **1998**, *12*, 345–348.

[8] K. Pervushin, R. Riek, G. Wider, K. Wuthrich, *Proc. Natl. Acad. Sci. USA* **1997**, *94*, 12366–12371.

[9] a) G. Bouvignies, P. Vallurupalli, L. E. Kay, *J. Mol. Biol.* **2014**, *426*, 763–774; b) D. Long, A. Sekhar, L. E. Kay, *J. Biomol. NMR* **2014**, *60*, 203–208; c) D. Long, G. Bouvignies, L. E. Kay, *Proc. Natl. Acad. Sci. USA* **2014**, *111*, 8820–8825.

[10] A. E. Eriksson, W. A. Baase, J. A. Wozniak, B. W. Matthews, *Nature* **1992**, *355*, 371–373.

[11] G. Bouvignies, P. Vallurupalli, D. F. Hansen, B. E. Correia, O. Lange, A. Bah, R. M. Vernon, F. W. Dahlquist, D. Baker, L. E. Kay, *Nature* **2011**, *477*, 111–114.

[12] F. A. A. Mulder, A. Mittermaier, B. Hon, F. W. Dahlquist, L. E. Kay, *Nat. Struct. Biol.* **2001**, *8*, 932–935.

[13] K. Tamiola, B. Acar, F. A. A. Mulder, *J. Am. Chem. Soc.* **2010**, *132*, 18000–18003.

[14] R. Ishima, D. A. Torchia, *J. Biomol. NMR* **2003**, *25*, 243–248.

Manuscript received: November 3, 2016
Revised: December 7, 2016
Final Article published: December 30, 2016

  